A Sensitivity Study of Daytime Net Radiation during Snowmelt to Forest Canopy and Atmospheric Conditions

JEAN EMMANUEL SICART,* JOHN W. POMEROY,+ RICHARD L. H. ESSERY,* JANET HARDY,#
TIMOTHY LINK,@ AND DANNY MARKS&

*Centre for Glaciology, Institute of Geography and Earth Sciences, University of Wales, Aberystwyth, Ceredigion, United Kingdom
+Department of Geography, University of Saskatchewan, Saskatoon, Saskatchewan, Canada
#U.S. Army ERDC Cold Regions Research and Engineering Laboratory, Hanover, New Hampshire
@Department of Forest Resources, University of Idaho, Moscow, Idaho
&Northwest Watershed Research Center, Agricultural Research Service, USDA, Boise, Idaho

(Manuscript received 7 November 2003, in final form 29 March 2004)

ABSTRACT

This study investigates the dependence of net radiation at snow surfaces under forest canopies on the overlying canopy density. The daily sum of positive values of net radiation is used as an index of the snowmelt rate. Canopy cover is represented in terms of shortwave transmissivity and sky-view factor. The cases studied are a spruce forest in the Wolf Creek basin, Yukon Territory, Canada, and a pine forest near Fraser, Colorado. Of particular interest are the atmospheric conditions that favor an offset between shortwave energy attenuation and longwave irradiance enhancement by the canopy, such that net radiation does not decrease with increasing forest density. Such an offset is favored in dry climates and at high altitudes, where atmospheric emissivities are low, and in early spring when snow albedos are high and solar elevations are low. For low snow albedos, a steady decrease in snowmelt energy with increasing canopy cover is found, up to a forest density close to the actual densities of mature spruce forests. Snowmelt rates for high albedos are either insensitive or increase with increasing canopy cover. At both sites, foliage area indices close to 2 are associated with a minimum in net radiation, independent of snow albedo or cloud cover. However, these results are more uncertain for open forests because solar heating of trees may invalidate the longwave assumptions, increasing the longwave irradiance.

1. Introduction

At high altitudes and latitudes, snow has a significant influence on hydrological and atmospheric processes. Large fractions of these regions are covered by evergreen coniferous forests. The retention of needles throughout the winter leads to a large influence of the canopy on snow accumulation and melting processes (e.g., Kuz'min 1972; Hedstrom and Pomeroy 1998; Lundberg et al. 1998; Ohta et al. 1999; Pomeroy and Dion 1996; Koivusalo and Kokkonen 2002).

Trees absorb a large part of the incoming shortwave radiation. During winter, when there is no tree transpiration, this heat load is dissipated as either a longwave radiation flux upward and downward or an upward and downward convective heat flux (Rouse 1984). Trees shelter the snow surface from wind, reducing turbulent fluxes, so subcanopy snowmelt depends mainly on the radiative fluxes (Price 1988). The magnitudes of net shortwave (positive) and net longwave (negative) radiative fluxes are reduced at the snow surface below a forest relative to open sites (Harding and Pomeroy 1996; Hardy et al. 1997). As canopy coverage increases, two competitive radiative changes affect snowmelt at the ground surface: vegetation attenuates the transmission of shortwave radiation but enhances longwave irradiance to the surface. The shortwave energy reduction is generally the dominant effect and melting is reduced (Link and Marks 1999). However, the longwave radiation increase may offset any reduction in shortwave irradiance, a situation that can be referred to as the ''radiative paradox'' defined by Ambach (1974).

Studies of the sensitivity of snowmelt to canopy coverage have generally been based on modeling results (Yamazaki and Kondo 1992; Davis et al. 1997), as the difficulty of observing different snowmelt rates under various canopy covers is large. Suzuki and Ohta (2003) simulated snowmelt rates under larch forests of different densities. Subcanopy variables such as solar irradiance, however, were empirically derived from the above-canopy atmospheric forcing; these statistical relations do not give much insight into the physical processes and are not necessarily stable over a broad range of forest densities.

Corresponding author address: Jean Emmanuel Sicart, Centre for Glaciology, Institute of Geography and Earth Sciences, University of Wales, Aberystwth, Ceredigion SY23 3DB, United Kingdom.
E-mail: jms@aber.ac.uk

TABLE 1. List of sensors used in the Wolf Creek forest with their specifications.

Quantity	Sensor type	Height (m)	Accuracy*
Air temperature	Vaisala HMP45, capacitive hygrothermometer	2, 15, 21	±0.2°C
Surface temperature	Everest, IR sensor, vertically above the canopy	2, 21	±0.5°C
Trunk temperature	Thermocouple	1	±0.1°C
Net radiation	REB net radiometer	21	±10%
	Delta-T tube net radiometer	2	±10%
Shortwave radiation	LI-COR LI-200SA pyranometer (upward)	21	±5%
	Matrix pyranometer (upward)	0	±5%
	Delta-T 1-m tube solarimeter (downward)	1.5	±5%
Longwave radiation	Eppley pyrgeometer	0	±10%

* According to the manufacturer.

This study examines the sensitivity of subcanopy net radiation components during snowmelt to canopy characteristics with reference to atmospheric conditions. Daytime fluxes are exclusively considered, since during nighttime the canopy limits longwave losses from the snow surface, and the snow temperature remains near the freezing point (e.g., Höller 2001). The dependence of subcanopy net radiation over snow to canopy characteristics is described in terms of shortwave transmissivity and sky-view factor. Of particular interest are the atmospheric conditions that favor an increase in net radiation under dense forests. The main case study is a spruce forest in the Wolf Creek basin, Yukon Territory, Canada. Data from a pine forest located near Fraser, Colorado, are used for comparison purposes.

2. Study sites and measurements

The primary study site was a subarctic forest in the Wolf Creek Research Basin, located 15 km south of Whitehorse (Yukon Territory, Canada; elevation: 750 m; 60°36′N, 134°57′W). A detailed description of the site can be found in Pomeroy et al. (2002). Observations were made in a dense forest of mature white spruce (*Picea glauca*), 12–18 m tall. From LI-COR LAI-2000 Plant Canopy Analyzer measurements (LI-COR 1992), Pomeroy et al. (2002) estimated the foliage area index, LAI′ (including clumping effects and stems, leaves, and branches), or ''effective LAI'' (Chen et al. 1997), to be 3.3 and the sky-view factor for the underlying snow surface to be 0.13.

The basin has a subarctic continental climate, characterized by a large annual variation in temperature, low humidity, and low precipitation. The mean annual temperature is approximately −3°C, with monthly mean temperatures ranging from 5° to 15° in summer and from −10° to −20°C in winter. The mean annual precipitation is around 350 mm, with approximately 40% falling as snow (Pomeroy and Granger 1997).

Measurements of air temperature (below, within, and above the canopy), canopy and ground surface temperatures, net radiation (above and below), and shortwave radiation (above and below) were made in April 2003 (Table 1). Incoming longwave radiation above the canopy was derived from measurements of downward-looking infrared surface temperature (primarily viewing the canopy, but also some ground), net radiation, and net shortwave radiation at a height of 21 m. Two Campbell dataloggers (21X and CR10) recorded 30-min averages of 5-s time step observations. Ten recently calibrated Matrix pyranometers were randomly located beneath the forest canopy to obtain a spatially integrated measure of incoming shortwave radiation at the snow surface. The subcanopy incoming longwave radiation was measured by two Eppley pyrgeometers placed on the snow surface. A separate measure of subcanopy net radiation using a Delta-T 1-m-tube net radiometer provided values very close to the net radiation calculated using the radiometer array, outgoing longwave radiation from the IR surface temperature, and reflected shortwave radiation measured using a downward-looking Delta-T 1-m-tube solarimeter.

Secondary observations were taken as part of the National Aeronautics and Space Administration's (NASA) Cold Land Processes Experiment (CLPX; http://www.nohrsc.nws.gov/~cline/clp.html) in a subalpine pine forest (40°N, 105°W; 2780 m MSL) in the U.S. Forest Service Fraser Experimental Forest near Fraser, Colorado. The mean annual temperature is approximately +0.5°C, and mean monthly temperatures are −10°C for January and +13°C for July, with an observed range of about −40° to +32°C (Alexander et al. 1985). The mean annual precipitation is about 750 mm, with nearly two-thirds falling as snow from October through May. The forest consists of logdepole pine (*Pinus contorta*) with an average height of 12.4 m (the ''uniform'' forest of Hardy et al. 2004). The sky-view factor below the canopy and the mean LAI′ were estimated to be 0.25 and 1.8 from hemispherical photographs and LI-COR LAI-2000 measurements, respectively.

An array of 10 Eppley pyranometers and 2 Eppley pyrgeometers was used to sample incoming radiation fluxes below the canopy (Rowlands et al. 2002). The incoming shortwave and longwave irradiances above the canopy were measured separately by a Kipp & Zonen CNR1 radiometer (accuracy: ±10% for daily sums), and the air temperature above the canopy was measured with

a Vaisala HMP45C hygrothermometer (accuracy: ±0.5°C). The measurement period used here is 27–29 March 2002.

3. Model

a. The radiation equation

Assuming that longwave radiation from canopy needles, stems, and trunks can be represented by a mean canopy temperature (T_c), the net all-wave radiation at the snow surface below a forest can be written as

$$R_n = V_f L_o\downarrow + (1 - V_f)\sigma T_c^4 - \sigma T_s^4 + K_o\downarrow \tau_c(1 - \alpha_s), \quad (1)$$

where V_f is the sky-view factor for the snow surface (the fraction of the celestial hemisphere visible from beneath the canopy), $L_o\downarrow$ is the above-canopy incoming longwave radiation, $\sigma = 5.67 \times 10^{-8}$ W m^{-2} K^{-4} is the Stefan–Boltzman constant, T_s is the snow surface temperature, $K_o\downarrow$ is the above-canopy incoming shortwave radiation (or global radiation), τ_c is the shortwave transmissivity of the canopy including multiple reflections ($\tau_c = K\downarrow/K_o\downarrow$, for shortwave irradiance $K\downarrow$ at the snow surface), and α_s is the snow albedo.

The longwave emissivities of vegetation and snow are generally considered to be close to $\varepsilon = 0.97$ (Mellor 1977; Oke 1987; Müller 1985; Dozier and Warren 1982). However, as Eq. (1) assumes that the snow and the vegetation surfaces are full emitters ($\varepsilon = 1$), reflection of longwave radiation by both surfaces may also be neglected ($\alpha = 1 - \varepsilon$ for opaque materials). This assumption is acceptable considering the accuracy of longwave radiation measurements and the desired simplicity of the radiative model used here. The time step is hourly. Only dense forests are considered to allow modeling of the canopy as a homogeneous horizontal scattering medium. The analysis does not deal with snow retained in the canopy since much of this will have dripped or evaporated by the spring, and Pomeroy and Dion (1996) showed that intercepted snow has a small influence on the shortwave transmissivity.

b. Sky-view factor and shortwave transmissivity

Subcanopy longwave irradiance can be written as

$$L\downarrow = V_f L_o\downarrow + (1 - V_f)\sigma T_c^4. \quad (2)$$

As the majority of the atmospheric longwave radiation ($L_o\downarrow$) received at the surface comes from the near-surface layer of the atmosphere, $L_o\downarrow$ may be written as

$$L_o\downarrow = \varepsilon_{\text{air}} \sigma T_{\text{air}}^4, \quad (3)$$

where ε_{air} is the apparent emissivity of the atmosphere, and T_{air} is the air temperature near the ground (Unsworth and Monteith 1975). Assuming that the mean canopy temperature is close to the air temperature ($T_c \approx T_{\text{air}}$; this assumption is discussed in section 4), the sensitivity of subcanopy longwave irradiance to changes in the sky-view factor can be written as a function of the atmospheric emissivity as

$$\Delta L\downarrow/L_o\downarrow = (1 - 1/\varepsilon_{\text{air}})\Delta V_f. \quad (4)$$

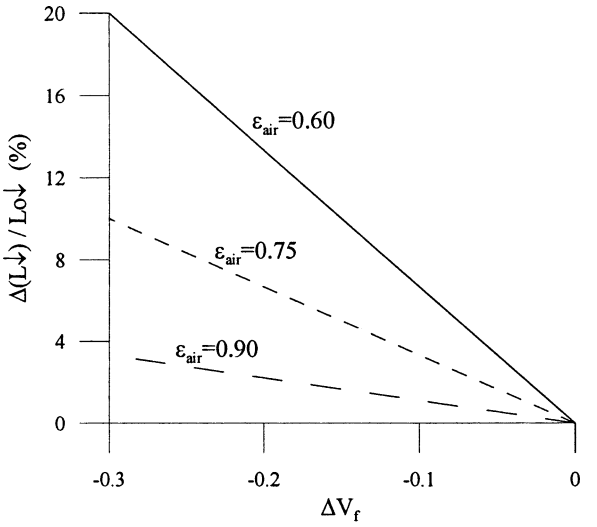

FIG. 1. Relative changes in incoming subcanopy longwave radiation caused by reductions in sky-view factor [Eq. (4)] for different atmospheric emissivities: $\varepsilon_{\text{air}} = 0.60$, 0.75, and 0.90.

Figure 1 shows changes in longwave radiation caused by reductions in the sky-view factor for three atmospheric emissivities. In mid- and high latitudes, the atmospheric emissivity ranges from 0.6 to 1 for clear to cloudy skies (Brutsaert 1982). The enhancement of longwave irradiance due to a sky-view factor reduction is maximal under clear skies (low atmospheric emissivity) but is independent of the forest density.

The accuracy of longwave radiation measurements is generally no better than ±10% (Halldin and Lindroth 1992). However, the main source of error is interference from solar radiation, so we can expect better accuracy under conditions of low solar radiation beneath a dense canopy. Figure 1 shows that uncertainties in V_f greater than ±0.05 may cause errors in longwave radiation calculations exceeding ±5% (under clear skies), that is, probably larger than the uncertainty in longwave measurements in a forested environment. This is an important point given the difficulty in ascertaining the accuracy of the canopy parameters.

We assume that the mean shortwave transmissivity is a monotonic increasing function of the sky-view factor,

$$V_f = f(\boldsymbol{\tau}_c). \quad (5)$$

As the shortwave transmissivity varies throughout the day with the solar angle, we define the daily average of transmissivity as

$$\boldsymbol{\tau}_c = \boldsymbol{K}\downarrow/\boldsymbol{K}_o\downarrow = \sum K\downarrow \Big/ \sum K_o\downarrow, \quad (6)$$

where the variables in bold italic are daily averages, and Σ notes the daily sum.

Various authors (e.g., Yamazaki and Kondo 1992; Gusev and Nasonova 2001) have assumed

$$V_f = \boldsymbol{\tau}_c. \tag{7}$$

Another relation between V_f and $\boldsymbol{\tau}_c$ can be derived from the empirical relationship that Pomeroy et al. (2002) observed between the sky-view factor and the foliage area index LAI′ from LI-COR LAI-2000 measurements in eight coniferous and deciduous forests in northern Canada ($r^2 = 0.97$):

$$V_f = a - b \ln(\text{LAI}'), \tag{8}$$

where $a = 0.45$ and $b = 0.29$ are constants. Shortwave transmissivity can be related to the foliage area index by Beer's law,

$$\tau_c = e^{-k\text{LAI}'}. \tag{9}$$

The extinction coefficient k is the average projected foliage area in the direction of the sun; k depends on the geometric and spectral properties of the incident radiation and the canopy. We define the mean extinction coefficient $\boldsymbol{k}$ as

$$\boldsymbol{k} = -\ln(\boldsymbol{\tau}_c)/\text{LAI}'. \tag{10}$$

Using Eqs. (8) and (10), the sky-view factor is related to the mean canopy shortwave transmissivity by

$$V_f = a - b \ln[-\ln(\boldsymbol{\tau}_c)/k]. \tag{11}$$

The total transmission of shortwave radiation results from the transmission of direct and diffuse above-canopy incoming radiation. Assuming a random distribution of leaves and a spherical foliage angle distribution, the extinction coefficient for direct radiation is

$$k_b = (2 \cos\theta)^{-1}, \tag{12}$$

where θ is the solar zenith angle. The penetration of direct solar radiation through the canopy is now

$$\tau_{c,b} = e^{-\text{LAI}'/(2 \cos\theta)} \tag{13}$$

The transmissivity ($\tau_{c,d}$) and the extinction coefficient (k_d) for diffuse radiation can be derived by numerical integration of the transmission for direct radiation over the entire hemisphere,

$$\tau_d = 2 \int_0^{\pi/2} \tau_b(\theta) \sin\theta \cos\theta \, d\theta. \tag{14}$$

The resulting k_d, constant throughout the day, generally depends on the foliage area index (Campbell and Norman 1998).

This simple model does not account for multiple scattering in the canopy or between the canopy and the forest floor, which tends to increase the shortwave irradiance at the snow surface (e.g., Nijssen and Lettenmaier 1999). The effect on snow albedo of potential changes in litter fallout under different canopy covers is not considered here either (Hardy et al. 2000).

c. Differentiation of the radiation equation

Replacing V_f in Eq. (1) by $f(\boldsymbol{\tau}_c)$, the derivative of the net radiation with respect to the shortwave transmissivity ($dR_n/d\boldsymbol{\tau}_c$) is zero when net radiation is independent of canopy density or when some canopy cover causes an optimum value of net radiation (maximum or minimum). We investigate the atmospheric conditions giving

$$dR_n/d\boldsymbol{\tau}_c = (L_o\downarrow - \sigma T_c^4) f'(\boldsymbol{\tau}_c) + K_o\downarrow(1 - \alpha_s) = 0, \tag{15}$$

where $f'(\boldsymbol{\tau}_c)$, the derivative of $f(\boldsymbol{\tau}_c)$, is 1 or $-b/[\boldsymbol{\tau}_c \ln\boldsymbol{\tau}_c]$ depending on whether $f(\boldsymbol{\tau}_c)$ is derived from Eqs. (7) or (11). Note that $\boldsymbol{k}$ does not appear in $f'(\boldsymbol{\tau}_c)$. Equation (15) assumes that $d\tau_c/d\boldsymbol{\tau}_c = 1$, that is, that the deviation of the hourly value from the average ($\tau_c - \boldsymbol{\tau}_c$) does not depend on the forest density. This assumption is probably incorrect for large changes in forest density since the diurnal cycle of τ_c increases in more open forests. However, the focus here is on dense forests, and we consider this assumption to be valid considering the simplicity of this study.

The first term in Eq. (15), representing the longwave flux, is generally negative as the canopy emissivity is greater than the atmospheric emissivity. The second term, representing the shortwave flux, is positive and is generally larger than the longwave term ($dR_n/d\boldsymbol{\tau}_c$ generally positive). Equation (15) permits quantification of the atmospheric conditions leading to an offset between the shortwave energy reduction and the longwave irradiance increase such that net radiation does not decrease with increasing forest density. For instance, at high altitude, high latitude, or in dry areas, atmospheric emissivity is low and so $L_o\downarrow$ is low; in early spring solar elevations are low and so is $K_o\downarrow$; and after fresh snowfall the subcanopy snow albedo is high.

Figure 2 compares the two expressions for $f'(\boldsymbol{\tau}_c)$ derived from Eqs. (7) and (11). For the logarithmic relation from Eq. (11), $f'(\boldsymbol{\tau}_c)$ becomes large for small shortwave transmissivities. Under very dense forests, Eq. (11) gives a rapid decrease in V_f, and hence an increase in subcanopy longwave irradiance, for only a small decrease in shortwave transmissivity. Compared to the linear relationship in Eq. (7), use of Eq. (11) reinforces the influence of longwave fluxes on the energy available for snowmelt, leading to more frequent situations of the ''radiative paradox'' where $dR_n/d\boldsymbol{\tau}_c \leq 0$.

4. Results

a. Air and canopy temperatures

The downward-looking radiant temperature of the canopy T_c integrates the emission of the vegetation elements at different heights [Eq. (2)]. In the Wolf Creek forest during snowmelt, the thermal gradient in the air below and above the canopy remained small during day-

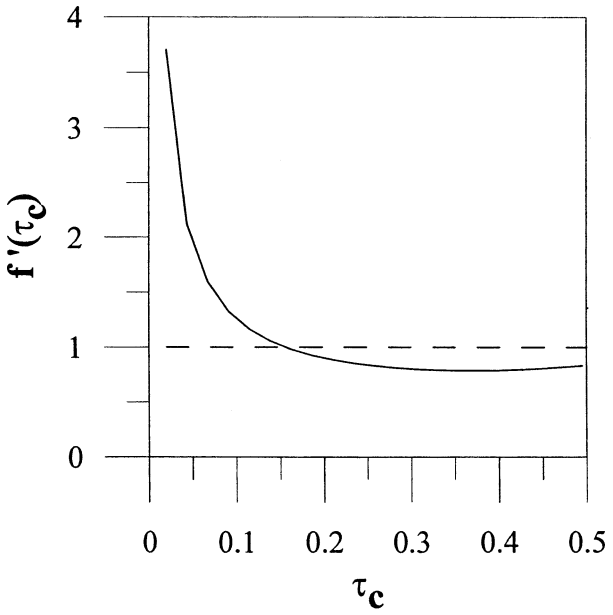

FIG. 2. Derivative $f'(\tau_c) = df(\tau_c)/d\tau_c$ of the relationship between V_f and τ_c from Eq. (7) (dashed line) and Eq. (11) (solid line).

time (Figs. 3a and 3b). The temperature of the vegetation at the top of the canopy remained close to the air temperature, whereas the lower trunks were colder than the air (Figs. 3c and 3d).

Under clear skies, the mean daytime longwave irradiance below the dense forest of Wolf Creek was enhanced by about 50% ($L_o\downarrow$ = 210 W m^{-2}; $L\downarrow$ = 320 W m^{-2}). The radiant canopy temperature (T_c), derived from measurements of subcanopy longwave irradiance [Eq. (2)], was similar to the above-canopy air temperature during daytime (r^2 = 0.94, slope 0.93, mean difference 1.2°C with an rms error of 1.9°C; Fig. 4). The errors in calculating subcanopy irradiance using T_{air} instead of T_c in Eq. (2) are small in the Wolf Creek forest: the mean difference is 6 W m^{-2} and the rms error is 10 W m^{-2} (Fig. 4).

b. Dependence of net radiation at the snow surface on canopy coverage

Daily sums of positive net radiation values at the snow surface were calculated as functions of the sky-view factor and shortwave transmissivity from mea-

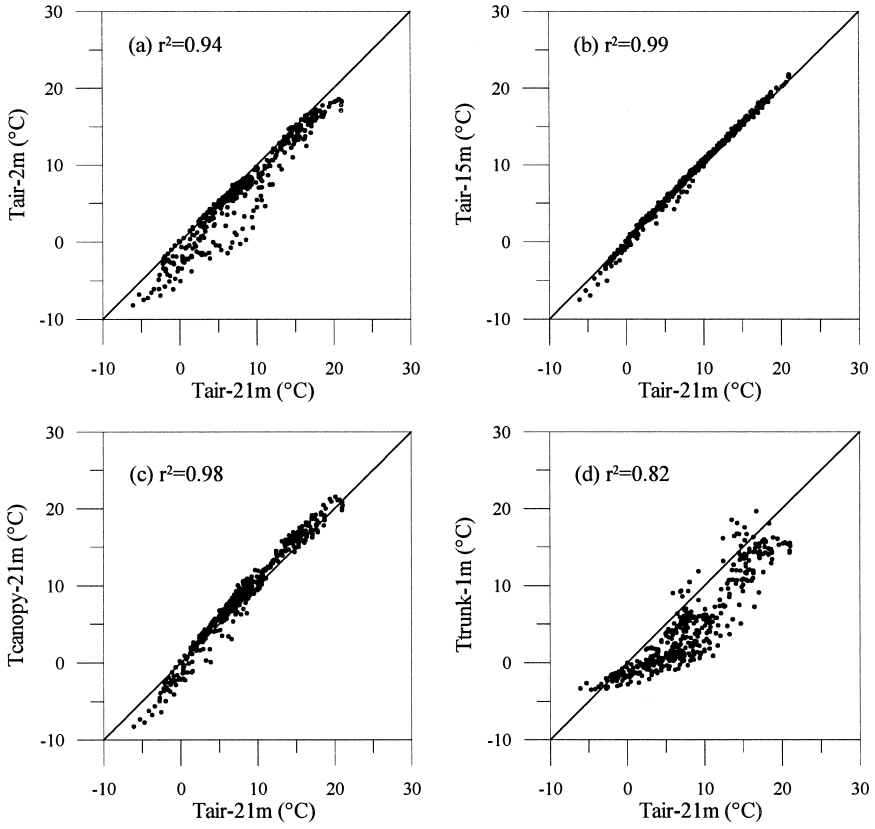

FIG. 3. Comparisons between half-hourly averages of daytime (0800–2000 LT) air and canopy temperatures for the Wolf Creek forest, 11–30 Apr 2003. Temperatures are plotted against the air temperature at 21-m height (the canopy height is 18 m). (a) Air temperature at 2-m height. (b) Air temperature at 15-m height. (c) Canopy-top temperature derived from infrared measurements. (d) Trunk temperature measured by thermocouples at a height of 1 m.

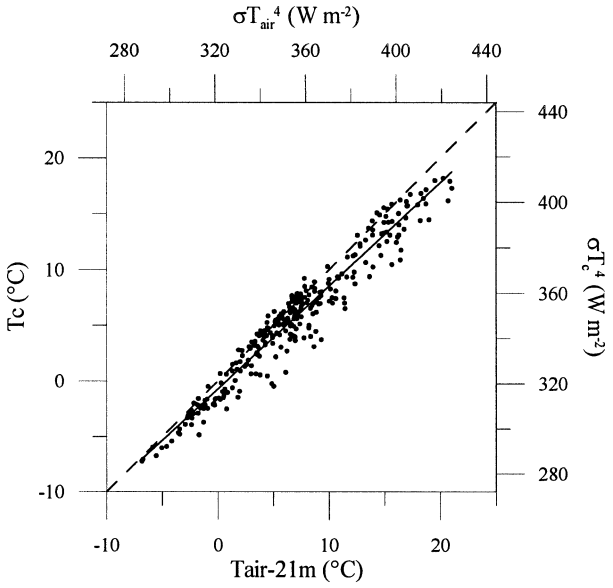

FIG. 4. Hourly averages of the air temperature at 21-m height and the canopy radiant temperature [T_c from Eq. (2)] during daytime (0800–2000 LT) for the Wolf Creek forest, 11–30 Apr 2003. The dashed line is the one-to-one line, and the solid line is the fit to the data.

surements of $L_o\downarrow$, T_{air}, and $K_o\downarrow$ in the Wolf Creek and Fraser forests (Figs. 5 and 6).

During the measurement periods, the minimum solar zenith angle at noon was around 50° in Wolf Creek and around 40° in Fraser. The shortwave transmissivity reached maximal values at midday of around 0.12 in Wolf Creek and 0.40 in Fraser; the overall averages were 0.06 (18 days) and 0.29 (only 3 days), respectively.

As separate measurements of diffuse and direct shortwave radiation were not available, one clear-sky day (mostly direct above-canopy solar irradiance) and one overcast day (mostly diffuse solar irradiance) were investigated for each site. For clear-sky conditions, the daily sums of net radiation were calculated on 13 April 2003 for Wolf Creek (measured snow albedo around 0.5) and on 28 March 2002 for Fraser (measured snow albedo around 0.8). The two relations between V_f and $\boldsymbol{\tau}_c$ derived from Eqs. (7) and (11) were used. The logarithmic relationship [Eq. (11)] requires considering the dependence of $\boldsymbol{\tau}_c$ and $\boldsymbol{k}$ on the foliage area index.

Figures 5b and 6b show that the Beer's law for penetration of direct shortwave radiation [Eq. (13)] gives a good approximation of the subcanopy incoming radiation at both sites when the sky is clear. Reduction of the extinction coefficient by a factor ranging from 0.51 to 0.85 (Campbell and Norman 1998; Nijssen and Lettenmaier 1999; Eagleson 2002) to account for multiple scattering in the canopy does not improve the agreement with the data (not shown). The largest errors in $K\downarrow$ are due to the underestimation of the maximum solar irradiance at noon for Fraser (by around 15%). We thus assume that the total transmission under a clear sky

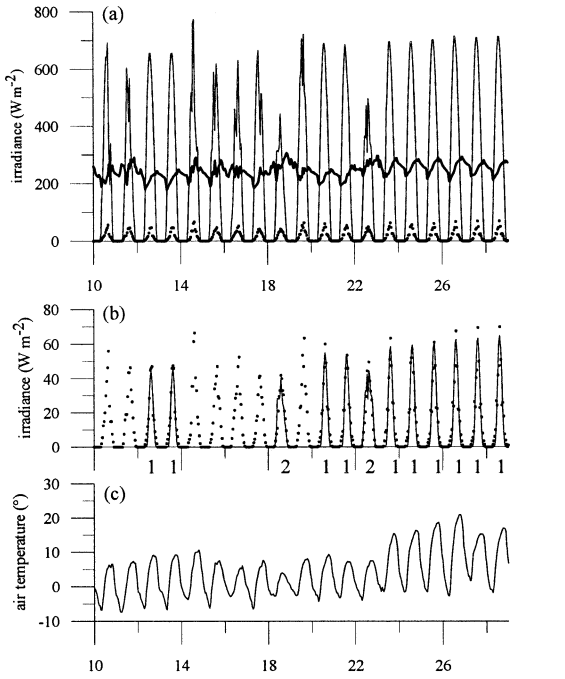

FIG. 5. Meteorological measurements in the Wolf Creek forest, 10–28 Apr 2003. (a) Above-canopy and subcanopy shortwave irradiances (solid line and dots, respectively), and above-canopy longwave irradiance (thick line). (b) Subcanopy shortwave irradiance measurements (dots) and calculations (solid line) according to Eq. (13) for clear-sky days (label 1) and Eq. (14) for overcast days (label 2). (c) Above-canopy air temperature.

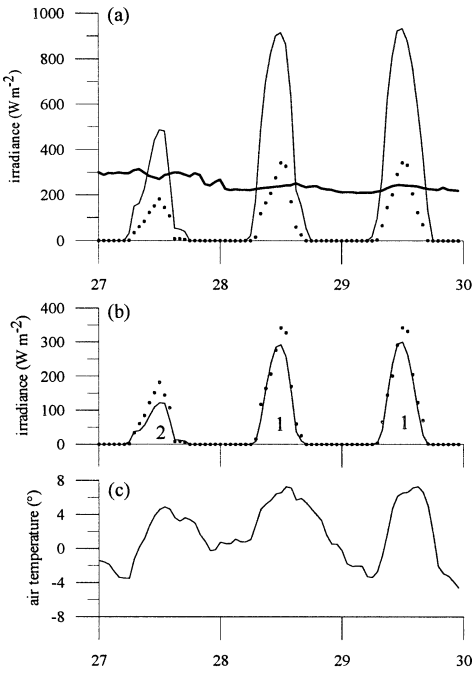

FIG. 6. As in Fig. 5, but for the Fraser forest, 27–29 Mar 2002.

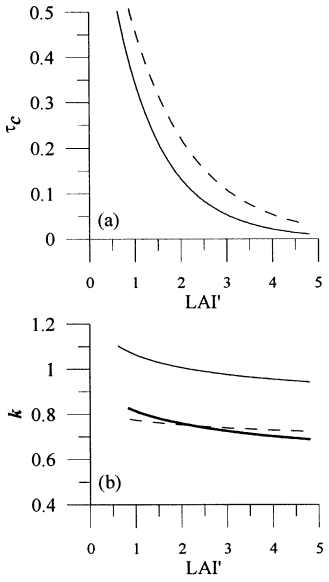

FIG. 7. Daily mean value of (a) shortwave transmissivity and (b) extinction coefficient for direct radiation according to foliage area index [Eqs. (10) and (16)] at Wolf Creek (solid line) and Fraser (dashed line). The thick line in (b) shows the extinction coefficient for diffuse radiation from Eq. (14).

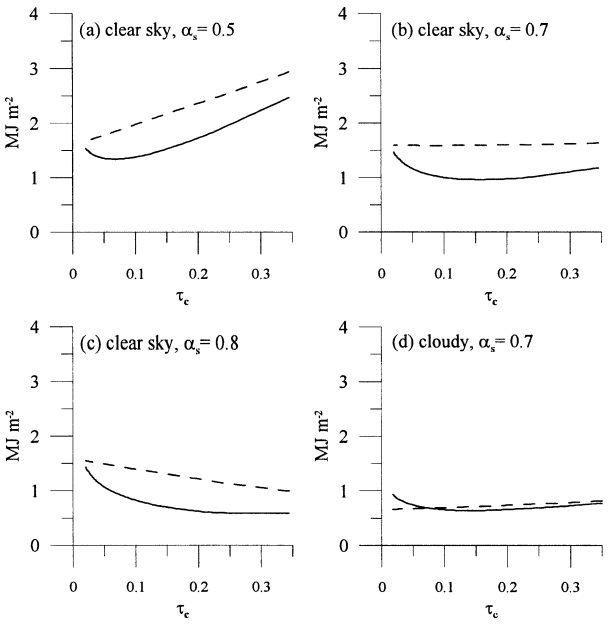

FIG. 8. Daily sums of positive values of net radiation as a function of the mean shortwave transmissivity (τ_c) for the Wolf Creek forest in spring 2003: 13 Apr (clear sky) with snow albedo (a) $\alpha_s = 0.5$, (b) $\alpha_s = 0.7$, and (c) $\alpha_s = 0.8$, respectively, and (d) 18 Apr (cloudy) with snow albedo $\alpha_s = 0.7$. The dashed line shows calculations with $V_f = \tau_c$, and the solid line shows calculations with $V_f = f(\tau_c)$ from Eq. (11).

($\tau_{c,\text{clear}}$) can be approximated by the transmission of direct radiation (τ_b) derived from Eq. (13), so Eq. (6) can be written as

$$\tau_{c,\text{clear}} \approx \tau_{c,b} = \frac{\int_\theta K_o\downarrow e^{-\text{LAI}'/(2\cos\theta)}\, d\theta}{\int_\theta K_o\downarrow\, d\theta}. \qquad (16)$$

The mean clear-sky extinction coefficient (k_{clear}) is then deduced from $\tau_{c,\text{clear}}$ through Eq. (10). Once $\tau_{c,\text{clear}}$ and k_{clear} are known, V_f is calculated from Eq. (11).

Figure 7 shows the dependence of $\tau_{c,\text{clear}}$ and k_{clear} on changes in foliage area index. The mean extinction coefficient does not change much with the forest density, remaining around 1.0 for Wolf Creek and 0.75 for Fraser (Fig. 7b). In the two cases studied, k_{clear} mainly depends on the properties of the above-canopy incident radiation and on structural properties of the canopy other than the foliage area index.

Figures 8a–c and 9a–c show the daily sums of positive values of net radiation under clear skies at Wolf Creek and Fraser, respectively. We only consider shortwave transmissivities larger than 0.02, which is close to the minimum value necessary for the growth of most plants in natural environments (Barnes et al. 1998). Assuming $\tau_c = V_f$ and a low snow albedo ($\alpha_s = 0.5$), the positive radiative energy steadily decreases as the forest is made denser for both sites (dashed lines, Figs. 8a and 9a), and no radiative offset appears. For a logarithmic relation between V_f and τ_c [Eq. (11)], a minimum in net radi-

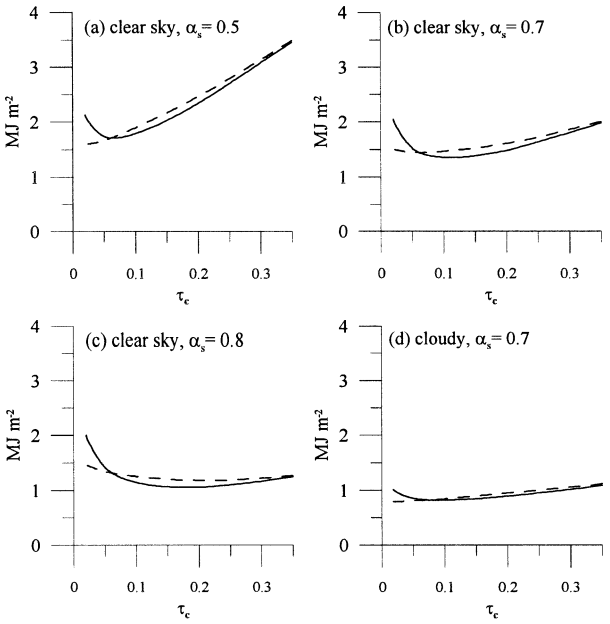

FIG. 9. As in Fig. 8, but for the Fraser forest in spring 2002: 28 Mar (clear sky) with snow albedo (a) $\alpha_s = 0.5$, (b) $\alpha_s = 0.7$, and (c) $\alpha_s = 0.8$, respectively, and (d) 27 Mar (cloudy) with snow albedo $\alpha_s = 0.7$.

ation occurs when the forest is very dense at a shortwave transmissivity of around 0.1 (solid lines, Figs. 8a and 9a). For higher snow albedos at Wolf Creek, positive values of snow net radiation become quite independent of canopy cover ($\alpha_s = 0.7$, Fig. 8b), or even increase with canopy cover for a clean snowpack ($\alpha_s = 0.8$, Figs. 8c). In Fraser, a minimum of net radiation still appears when $\alpha_s = 0.7$ (Fig. 9b), and positive values of snow net radiation do not change much with canopy density for higher snow albedo ($\alpha_s = 0.8$, Fig. 9c).

The transmissivity for diffuse radiation calculated from Eq. (14) is close to the measurements of total transmissivity during cloudy days at Wolf Creek ($\tau_d = 0.09$, Fig. 5b) and Fraser ($\tau_d = 0.25$, Fig. 6b). As above-canopy solar irradiance is mostly diffuse under an overcast sky, the transmissivity and the extinction coefficient were taken equal to τ_d and k_d, respectively, and calculated as functions of LAI′ only through Eq. (14). As a result, Fig. 7b shows that k_d is very close to $\boldsymbol{k}_{\text{clear}}$ for Fraser.

Figures 8d and 9d show the daily sums of net radiation during two cloudy days: 18 April (Wolf Creek) and 27 March (Fraser). At both sites, the daily above-canopy shortwave irradiance was around 35% of the irradiance at the top of the atmosphere, which is close to the minimum value observed in spring at Wolf Creek. In the calculations, the snow albedo was fixed at 0.7 as an intermediate value. For both sites and both assumed relationships between V_f and $\boldsymbol{k}$, the daily sum of radiation energy does not change much with forest density (Figs. 8d and 9d).

c. Sensitivity of net radiation to snow albedo

The threshold albedo above which positive net radiation increases with decreasing canopy transmissivity (increasing forest cover) is α_t such that $dR_n/d\boldsymbol{\tau}_c \leq 0$ when $\alpha \geq \alpha_t$. Presuming Eq. (11), α_t can be solved from Eq. (15):

$$\alpha_t = 1 - b\,(L_o\downarrow - \sigma\, T_c^4)/(K_o\downarrow\, \boldsymbol{\tau}_c\, 1\text{n}\boldsymbol{\tau}_c). \quad (17)$$

Figure 10 shows calculations of $dR_n/d\boldsymbol{\tau}_c$ derived from observations in the Wolf Creek and Fraser forests during melt periods at midday, when incoming energy at the snow surface is maximal; $dR_n/d\boldsymbol{\tau}_c$ depends more on the snow albedo than on the shortwave transmissivity since the dependence of R_n on $\boldsymbol{\tau}_c$ includes the enhancement of longwave irradiance with increasing canopy density [Eq. (15)]. At both sites, α_t becomes quite independent of the shortwave transmissivity when $\boldsymbol{\tau}_c$ is greater than 0.2. In the Wolf Creek forest ($\boldsymbol{\tau}_c$ around 0.06), α_t is around 0.55 when the sky is clear (Fig. 10a) and around 0.68 when the sky is cloudy (Fig. 10b). In the Fraser forest ($\boldsymbol{\tau}_c$ around 0.29), α_t is around 0.90 when sky is the clear (Fig. 10c) and around 0.85 when the sky is cloudy (Fig. 10d). The albedo threshold α_t is higher at Fraser than at Wolf Creek because of the lower latitude, which leads to higher shortwave irradiance [Eq. (17)].

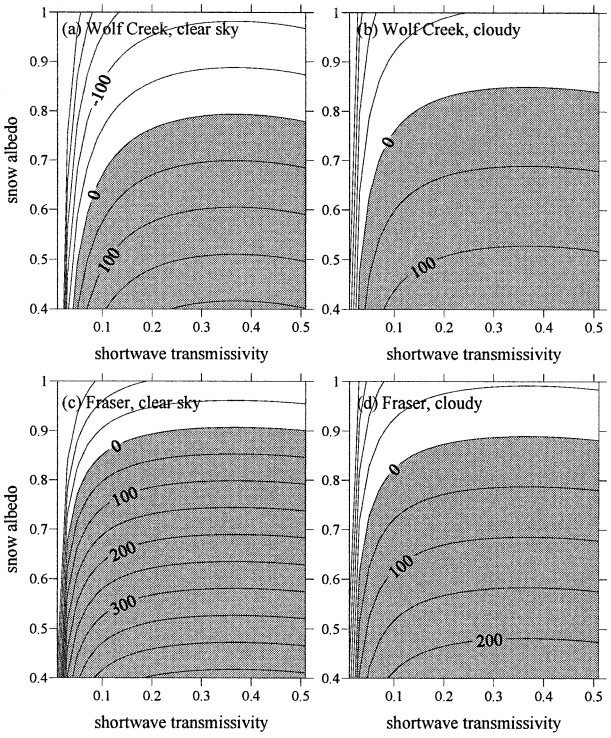

FIG. 10. Derivatives of the net radiation ($dR_n/d\boldsymbol{\tau}_c$ in W m^{-2}) as functions of shortwave transmissivity and snow albedo [Eq. (15) with $f'(\boldsymbol{\tau}_c) = -b/(\boldsymbol{\tau}_c \ln\boldsymbol{\tau}_c)$]. Hourly average values at 1200 LT in the Wolf Creek forest on (a) 13 Apr (clear sky) and (b) 18 Apr (cloudy), and hourly average values at 1200 LT in the Fraser forest on (c) 28 Mar (clear sky) and (d) 27 Mar (cloudy). Areas of positive $dR_n/d\boldsymbol{\tau}_c$ are shaded. The zero contour gives the threshold albedo as a function of $\boldsymbol{\tau}_c$ (see text).

5. Discussion

The sky-view factor controls the apportionment of subcanopy longwave irradiance originating from the atmosphere and from the vegetation [Eq. (2)]. It can be measured by fish-eye photography or indirectly derived from radiation measurements (Welles 1990). A sensitivity study suggests that the required accuracy in the sky-view factor is about ± 0.05, whatever the forest density. High accuracy is crucial in dry climates characterized by low atmospheric emissivities.

From the equation of net radiation, atmospheric conditions that cause an offset between shortwave energy attenuation and longwave irradiance enhancement by the canopy were quantified. Such an offset is favored in dry climates and at high altitudes and latitudes, where atmospheric emissivities are low, and in early spring when snow albedo is high and solar elevation is still low. These atmospheric conditions favor higher net radiation when moving from sparse to dense canopies while all other conditions are unchanged. However, for a fixed canopy density, net radiation at the snow surface is still higher for higher incoming longwave or shortwave radiation or lower snow albedo.

The radiant canopy temperature T_c was deduced from

longwave irradiances below and above the canopy [Eq. (2)]. In Wolf Creek, T_c was slightly lower than the air temperature above the canopy, but the difference remained small (1.2°C on average; Fig. 4). A large part of the longwave emission by the canopy probably originates from needles and small branches in thermal equilibrium with the air. Below the canopy at Wolf Creek, trunks are shaded and are generally colder than the air during daytime. During snowmelt in dense high-latitude coniferous forests, air temperature can therefore be used as a substitute for the canopy radiant temperature. In more open forests, like Fraser, trunks tend to be more heated by direct shortwave radiation, causing large temperature differences between vegetation and air at low wind speeds (Otterman et al. 1988; Rowlands et al. 2002), which may lead to large errors in calculations of $L\downarrow$ assuming $T_c = T_{\text{air}}$. However, the focus here is on climates (early spring) and canopy properties (dense forests) that favor the occurrence of the ''radiative paradox'': these conditions also favor small differences between T_{air} and T_c. In Fraser, the atmospheric data were used to simulate the net radiation below hypothetical forests denser than the real one.

Two relationships between the sky-view factor and the mean shortwave transmissivity of the canopy were considered: the equality $V_f = \boldsymbol{\tau}_c$ and a logarithmic relation derived from LI-COR LAI-2000 measurements by Pomeroy et al. (2002) in eight boreal forests [Eq. (11)]. However, the LAI-2000 derives the sky-view factor beneath the canopy and the foliage area index from measurements of the transmitted blue sky light (wavelengths 400–490 nm; Welles and Norman 1991). Thus, Eq. (11) may be influenced by the calculations performed by the LAI-2000 software.

Assuming a random distribution of leaves with a spherical angle distribution, the hourly values of transmissivity in direct radiation were calculated from foliage area index and solar zenith angle through a Beer's law relationship [Eq. (13)]. The spherical assumption is probably not correct for all coniferous forests (e.g., Black et al. 1991). However, this assumption allows simple calculations whose results are roughly in agreement with the observations in both cases studied, for both clear and cloudy conditions (Figs. 5 and 6). The spherical foliage angle distribution is also in agreement with LAI-2000 measurements of the canopy ''mean tilt angle'' (MTA) in the Wolf Creek forest: MTA = 59° ± 6° (n = 12).

At both sites, the observed shortwave transmissivity of the canopy in clear-sky conditions is close to the calculated transmissivity for direct radiation (Figs. 5 and 6). The main deviations from Beer's law occur around noon at Fraser (Fig. 6). This discrepancy may come from canopy heterogeneities in the rather open Fraser forest: low solar zenith angles can give direct illumination of large ground areas, violating the basic assumptions of Beer's law. Indeed, pyranometer measurements at 5-min time steps show peaks of direct illumination around noon. For averaged radiation data, however, errors in using Beer's law remain low (about 15%).

The daily extinction coefficient for direct radiation does not depend much on the foliage area index (Fig. 7b). The extinction coefficient is higher at the northern site (Wolf Creek, $\boldsymbol{k}_{\text{clear}} \approx 1$) than at the southern site (Fraser, $\boldsymbol{k}_{\text{clear}} \approx 0.75$) because the spherical angle distribution of leaves intercepts more radiation at a large zenith angle (Campbell and Norman 1998). As a result, in the spring climate of Wolf Creek, a canopy cover increase causes a steady decrease in snowmelt when the snow albedo is low, up to a density close to the actual density of the studied spruce forest (Fig. 8). Large snow albedo values cause a low dependence of snowmelt on canopy cover or a steady increase in melt energy when the canopy cover increases (Fig. 8). The results are similar for Fraser, but, because of more southerly latitude, shortwave irradiance is higher, such that offsets between decreases of shortwave transmissivity and enhancement of longwave subcanopy irradiance are less likely (Fig. 9). These results are more uncertain for large shortwave transmissivities (more open forests) because solar heating of trees may invalidate the longwave assumptions, increasing the long wave above the estimates.

In Wolf Creek, the daily sum of net radiation, which is directly related to the snowmelt, depends on the functional form of $f(\boldsymbol{\tau}_c)$, giving differences in R_n of up to a factor of 2 (Fig. 8). Thus, in canopy radiative models, the choice of the relation between V_f and $\boldsymbol{\tau}_c$, which depends both on climate and canopy structural properties, may have a strong impact on snowmelt calculations.

With the logarithmic relation for $V_f = f(\boldsymbol{\tau}_c)$, a minimum in net radiation seems to occur under clear and cloudy conditions, independent of the snow albedo, when the shortwave transmissivity is around 0.15, corresponding to LAI′ ≈ 1.9 and 2.5 in Wolf Creek and Fraser, respectively (Figs. 8 and 9).

The net radiation equation was differentiated with respect to the shortwave transmissivity in order to study the sensitivity of snowmelt to the snow albedo under the canopy. When snow albedo exceeds a threshold (α_t), the longwave irradiance enhancement by the canopy can potentially offset the shortwave energy reduction. In the Wolf Creek climate, the albedo threshold α_t ranges from 0.5 to 0.7, depending on cloud cover. In Fraser, the albedo threshold remains high (around 0.9) because of high shortwave irradiance at this more southerly site. Any increase in above-canopy longwave irradiance reduces the effects of longwave emission by the canopy, such that situations of ''radiative paradox'' are not favored and α_t tends to increase. Cloud cover causes both a reduction in incoming shortwave energy and an increase in atmospheric emissivity, with countering effects on α_t. The overall effect of clouds on the threshold albedo α_t depends on climatic conditions.

Snowmelt or net radiation measurements under various canopy covers, but under the same climatic forcing,

are not frequent. In Japan (42°N), Ohta et al. (1999) observed only small changes in net radiation at the snow surface below three coniferous and deciduous forests ($LAI' = 0.87$, 1.73, and 6.00). In the same climatic environment, Suzuki and Ohta (2003) did not observe significant differences in snowmelt rates under sparse ($LAI' = 0.48$) and dense ($LAI' = 1.05$) larch forests. Similarly, but in a different climate, Petzold (1981) observed that the net radiation at the snow surface below three boreal forests only depends a little on forest density. Pomeroy and Granger (1997) observed little difference in available melt energy between different Canadian boreal forests: jack pine (two sites, $LAI' = 2.2$ and 0.8) and mixed wood (aspen and white spruce, $LAI' = 0.4$). These examples are roughly in agreement with the general offset between decrease in shortwave transmissivity and enhancement of subcanopy longwave irradiance by the canopy shown in this sensitivity study based on physical considerations.

6. Conclusions

This study examined the sensitivity of subcanopy net radiation components during snowmelt to canopy characteristics with reference to atmospheric conditions. A simple model was derived from meteorological observations in a spruce forest in the Yukon Territory, Canada (60°N), and in a pine forest in Colorado (40°N). As the snow surface beneath a canopy is not greatly cooled during the night, the daily sum of the positive values of the net radiation was used as an index of the snowmelt rate. The dependence of subcanopy net radiation over snow to canopy characteristics was described in terms of mean shortwave transmissivity and sky-view factor.

It was found that the daily net radiation at the snow surface under dense coniferous boreal forests does not depend much on the canopy density when the snow is clean (albedo > 0.5): the enhancement of subcanopy longwave irradiance as canopy density increases generally compensates for the decrease of shortwave transmissivity. In both cases studied, foliage area indices close to 2 (shortwave transmissivity around 0.15 and sky-view factor around 0.2) seem to be associated with a minimum of daily net radiation, independent of snow albedo or cloud cover.

Acknowledgments. The authors would like to thank all those who contributed to the field experiments, especially Newell Hedstrom and Raoul Granger (Environment Canada), Dan Bewley and Aled Rowlands (University of Wales), Rick Janowicz, Glen Ford, and Glen Carpenter (Yukon Environment), Kelly Elder and Manuel Martinez (U.S. Forest Service), and Gerald Flertchinger and Adam Winstral (USDA, ARS). Wolf Creek Research Basin is operated by the Water Resources Branch, Yukon Department of Environment and National Water Research Institute, Environment Canada; Fraser Experimental Forest is operated by the Rocky Mountain Research Station, U.S. Forest Service, and data was collected there as part of NASA's Cold Land Processes Mission, directed by Dr. Don Cline. Funding to support this study was provided by the U.K. Natural Environment Research Council, the U.S. National Oceanographic and Atmospheric Administration GEWEX Americas Prediction Project, the U.S. Army CRREL, the Canadian Foundation for Climate and Atmospheric Studies, the National Water Research Institute of Environment Canada, and the U.K. Strategic Research Investment Fund through the University of Wales, Aberystwyth. The authors are also grateful to three anonymous reviewers and to the editor for making very useful comments on the manuscript.

REFERENCES

Alexander, R. A., C. A. Troendel, M. R. Kaufmann, W. D. Shepperd, G. L. Crouch, and R. K. Watkins, 1985: The Fraser Experimental Forest, Colorado: Research program and published research 1937–1985. USDA Forest Service General Tech. Rep. RM-118, 46 pp.

Ambach, W., 1974: The influence of cloudiness on the net radiation balance of a snow surface with high albedo. *J. Glaciol.*, **13,** 73–84.

Barnes, B. V., D. R. Zak, S. R. Denton, and S. H. Spurr, 1998: *Forest Ecology*. Wiley, 774 pp.

Black, T. A., J. M. Chen, L. Xuhui, and R. M. Sagar, 1991: Characteristics of shortwave and longwave irradiances under a Douglas-fir forest stand. *Can. J. For. Res.,* **21,** 1020–1028.

Brutsaert, W., 1982: *Evaporation into the Atmosphere: Theory, History, and Applications.* Kluwer, 299 pp.

Campbell, G. S., and J. M. Norman, 1998: *An Introduction to Environmental Biophysics.* Springer, 285 pp.

Chen, J. M., P. M. Rich, S. T. Gower, J. M. Norman, and S. Plummer, 1997: Leaf area index of boreal forests: Theory, techniques, and measurements. *J. Geophys. Res.,* **102,** 29 429–29 443.

Davis, R. E., J. P. Hardy, W. Ni, C. E. Woodcock, J. C. McKenzie, R. Jordan, and X. Li, 1997: Variation of snow cover ablation in the boreal forest: A sensitivity study on the effects of conifer canopy. *J. Geophys. Res.*, **102,** 29 389–29 395.

Dozier, J., and S. G. Warren, 1982: Effect of viewing angle on the infrared brightness temperature of snow. *Water Resour. Res.*, **18,** 1424–1434.

Eagleson, P. S., 2002: *Ecohydrology.* Cambridge University Press, 443 pp.

Gusev, E. M., and O. N. Nasonova, 2001: Parameterization of heat and moisture transfer processes in ecosystems of boreal forests. *Atmos. Oceanic Phys.*, **37,** 167–185.

Halldin, S., and A. Lindroth, 1992: Errors in net radiometry: Comparison and evaluation of six radiometer designs. *J. Atmos. Oceanic Technol.*, **9,** 762–783.

Harding, R. J., and J. W. Pomeroy, 1996: The energy balance of the winter boreal landscape. *J. Climate,* **9,** 2778–2787.

Hardy, J. P., R. E. Davis, R. Jordan, X. Li, C. E. Woodcock, W. Ni, and J. C. McKenzie, 1997: Snow ablation modeling at the stand scale in a boreal jack pine forest. *J. Geophys. Res.*, **102,** 29 397–29 405.

——, R. A. Melloh, P. Robinson, and R. Jordan, 2000: Incorporating effects of forest litter in a snow process model. *Hydrol. Processes,* **14,** 3227–3237.

——, ——, D. Marks, G. Koenig, J. Pomeroy, and T. Link, 2004: Solar radiation transmission through conifer canopies. *Agric. For. Meteor.*, in press.

Hedstrom, N. R., and J. W. Pomeroy, 1998: Measurements and modeling of snow interception in the boreal forest. *Hydrol. Processes,* **12,** 1611–1625.

Höller, P., 2001: The influence of the forest on night-time snow surface temperature. *Ann. Glaciol.*, **32,** 217–222.
Koivusalo, H., and T. Kokkonen, 2002: Snow processes in a forest clearing and in a coniferous forest. *J. Hydrol.*, **262,** 145–164.
Kuz'min, P. P., 1972: *Melting of Snow Cover*. Israel Program for Scientific Translations, 345 pp.
LI-COR, 1992: LAI-2000 plant canopy analyzer. LI-COR Instruction Manual, 80 pp.
Link, T., and D. Marks, 1999: Point simulation of seasonal snow cover dynamics beneath boreal forest canopies. *J. Geophys. Res.*, **104,** 27 841–27 857.
Lundberg, A., I. Calder, and R. Harding, 1998: Evaporation of intercepted snow: Measurements and modelling. *J. Hydrol.*, **206,** 151–163.
Mellor, M., 1977: Engineering properties of snow. *J. Glaciol.*, **19,** 15–99.
Müller, H., 1985: Review paper: On the radiation budget in the Alps. *J. Climatol.*, **5,** 445–462.
Nijssen, B., and D. P. Lettenmaier, 1999: A simplified approach for predicting shortwave radiation transfer through boreal forest canopies. *J. Geophys. Res.*, **104,** 27 859–27 868.
Ohta, T., K. Suzuki, Y. Kodama, J. Kubota, Y. Kominami, and Y. Nakai, 1999: Characteristics of the heat balance above the canopies of evergreen and deciduous forests during the snowy season. *Hydrol. Processes,* **13,** 2383–2394.
Oke, T. R., 1987: *Boundary Layer Climates*. Routledge, 435 pp.
Otterman, J., K. Staenz, K. Itten, and G. Kukla, 1988: Dependence of snow melting and surface–atmosphere interactions on the forest structure. *Bound.-Layer Meteor.,* **45,** 1–8.
Petzold, D. E., 1981: The radiation balance of melting snow in open boreal forest. *Arct. Alp. Res.,* **13,** 287–293.
Pomeroy, J. W., and K. Dion, 1996: Winter radiation extinction and reflection in a boreal pine canopy: Measurements and modelling. *Hydrol. Processes,* **10,** 1591–1608.
——, and R. J. Granger, 1997: Sustainability of the western Canadian boreal forest under changing hydrological conditions. I. Snow accumulation and ablation. *Proc. Rabat Symp.*, Rabat, Morocco, IAHS Publ. 240, 237–242.
——, D. M. Gray, N. R. Hedstrom, and J. R. Janowicz, 2002: Prediction of seasonal snow accumulation in cold climate forests. *Hydrol. Processes,* **16,** 3543–3558.
Price, A. G., 1988: Prediction of snowmelt rates in a deciduous forest. *J. Hydrol.*, **101,** 145–157.
Rouse, W. R., 1984: Microclimate at the arctic tree line. 1. Radiation balance of tundra and forest. *Water Resour. Res.*, **20,** 57–66.
Rowlands, A., J. W. Pomeroy, J. Hardy, D. Marks, K. Elder, and R. Melloh, 2002: Small-scale spatial variability of radiant energy for snowmelt in a mid-latitude sub-alpine forest. *Proc. 59th Eastern Snow Conf.*, Stowe, VT, Eastern Snow Conference, 109–117.
Suzuki, K., and T. Ohta, 2003: Effect of larch forest density on snow surfaces energy balance. *J. Hydrometeor.*, **4,** 1181–1193.
Unsworth, M. H., and J. L. Monteith, 1975: Geometry of long-wave radiation at the ground, I. Angular distribution of incoming radiation. *Quart. J. Roy. Meteor. Soc.*, **101,** 13–24.
Welles, J. M., 1990: Some indirect methods of estimating canopy structure. *Remote Sens. Rev.*, **5,** 31–43.
——, and J. M. Norman, 1991: Instrument for indirect measure of canopy structure. *Agronomy J.*, **5,** 818–825.
Yamazaki, T., and J. Kondo, 1992: The snowmelt and heat balance in snow-covered forested areas. *J. Appl. Meteor.*, **31,** 1322–1327.